Modeling Earth Systems and Environment (2025) 11:328
https://doi.org/10.1007/s40808-025-02516-7

ORIGINAL ARTICLE

Enhancing drought trend analysis in northeastern Algeria with integrated classification frequencies for deeper insights

Amina Amarchi[1] · Lotfi Zeghadnia[2] · Moncef Chabi[1] · Hocine Amarchi[1] · Fares Laouacheria[1]

Received: 9 April 2025 / Accepted: 29 June 2025

Abstract
As a widespread environmental phenomenon, drought exerts significant adverse effects on agricultural productivity and environmental stability. Thorough drought assessment is essential for effective water resource management and monitoring strategies. Traditionally, drought is analyzed temporally and spatially without accounting for trend evolution, though trend studies have gained traction recently. This research addresses this gap by examining trend shifts, including frequency variations of drought classifications and their intensities, using a hybrid Frequency Innovative Trends and Statistics Analysis (FITA) and Innovative Trend Analysis (ITA) approach. The study applies 12-month Standardized Precipitation Index (SPI12), Reconnaissance Drought Index (RDI12), and Streamflow Drought Index (SDI12) across 10 stations in northeastern Algeria 1975–2021. Findings reveal that FITA-ITA enhances drought trend evaluation by offering a detailed microscale analysis of meteorological and hydrological patterns beyond simple increases or decreases. For instance, El Kalla shows a 100% increasing SPI12 trend (ITA slope 1.160), while Khenchela exhibits a 100% decreasing SPI12 trend (ITA slope −0.846). At Medjaz Amar, SDI12 increases 100% (ITA slope 0.797) despite an 82.61% decreasing RDI12 (ITA slope −1.294), reflecting streamflow gains amid agricultural droughts. These trends signal heightened risks to groundwater, desertification, and aquatic ecosystems, emphasizing the need for adaptive measures like rainwater harvesting and early warning systems to strengthen resilience in this semi-arid Mediterranean region.

Keywords Drought trends · FITA analysis · ITA slopes · Northeastern Algeria · Drought indices · Environmental dynamics

Introduction

Drought, a multifaceted natural hazard, severely affects water resources, agriculture, and ecosystems, especially in semi-arid areas such as northeastern Algeria (Wilhite and Pulwarty 2017; Vicente-Serrano et al. 2010). Defined by extended periods of reduced precipitation, droughts disrupt hydrological and socio-economic systems, requiring advanced monitoring and modeling techniques (Hassanein et al. 2013).

Understanding drought entails acknowledging its varied effects, shaped by unique categories influencing different environmental facets. Meteorological drought, signaled by diminished rainfall, highlights early water deficits but might miss later climatic shifts. Agricultural drought, fueled by reduced soil moisture and water loss through plants, indicates crop hardship, though its evaluation can struggle with erratic weather data across some areas. Hydrological drought, linked to lowered river flows, points to water

✉ Lotfi Zeghadnia
lotfi.zeghadnia@univ-soukahras.dz

Amina Amarchi
amina.amarchi@univ-annaba.dz

Moncef Chabi
moncef.chabi@univ-annaba.dz

Hocine Amarchi
hocine.amarchi@univ-annaba.dz

Fares Laouacheria
fars.laouacheria@gmail.com

1 Laboratory of Soil and Hydraulic, Department of Hydraulic, Faculty of Technology, Badji Mokhtar Annaba University, 23000 Annaba, Algeria

2 Laboratory of Modeling and Socio-Economic Analysis in Water Science "MASESE", University of Souk Ahras, 41000 Souk Ahras, Algeria

Published online: 08 July 2025

availability concerns, yet its assessment may face hurdles due to limited stream monitoring.

In Algeria, persistent drought conditions since the 1970s, marked by decreasing rainfall and increasing temperatures, have intensified water scarcity and environmental risks (Mostafa-Kara 2013; Khoualdia et al. 2014; AMARD 2014; Denidina et al. 2020; Elouissi et al. 2021; Haied et al. 2023; IPCC 2019; Mohammed and Al-Amin 2018; Essa et al. 2023). The global increase in drought frequency underscores the need for reliable models to predict and mitigate its impacts. Several approaches have been proposed, including probabilistic models for joint drought characteristics, neural-based forecasting, and hybrid methods integrating climatic indices with remote sensing data (Cancelliere et al. 2007; Morid et al. 2007; Kim and Valdes 2003; Mishra and Singh 2011; Yisehak and Zenebe 2021), Machine learning models, such as multilayer perceptrons and random forests, enhance forecasting accuracy, (Alkubaisi et al. 2025; Hakam et al. 2023; Pham et al. 2022; Ihinegbu and Ogunwumi 2022; Habibi et al. 2024; Kesgin et al. 2024).

Assessing drought severity is complex due to its diverse characteristics, necessitating indices like the Standardized Precipitation Index (SPI) for meteorological drought, the Reconnaissance Drought Index (RDI) for agricultural drought, and the Streamflow Drought Index (SDI) for hydrological drought (Quiring 2009; Djebou 2017; Jahangir et al. 2024; McKee et al. 1993; Tsakiris and Vangelis 2005; Hayes et al. 2011; WMO 2016; Turhan and Değerli Şimşek 2023; Nalbantis and Tsakiris 2009). Other indices include the Palmer Drought Severity Index (PDSI); the Surface Water Supply Index (SWSI); the Reclamation Drought Index (RCDI); the Standardized Precipitation Evapotranspiration Index (SPEI); and the Actual Precipitation Index (API) (Palmer 1965; Shafer and Dezman 1982; Vicente-Serrano et al. 2010). Climate change exacerbates drought intensity and frequency through rapid variations in temperature and precipitation, underscoring the importance of trend analysis (IPCC 2019). Conventional trend analysis methods, such as the Mann–Kendall test, rely on restrictive assumptions (e.g., data normality), limiting their suitability for non-stationary climate data (Mann 1945; Kendall 1975; Şen 2012; Kenabatho 2025). To address these constraints, Şen (2012) introduced the Innovative Trend Analysis (ITA), a nonparametric approach that identifies trends via subseries comparisons, widely used in hydroclimatic research. This paper presents the Frequency Innovative Trends and Statistics Analysis (FITA) as the original model, developed by Abu Arra et al. (2024), which advances ITA by integrating spectral frequency analysis to quantify drought classification frequencies (e.g., mild, moderate, severe). Unlike ITA's focus on monotonic trends, FITA detects cyclic patterns and severity distributions, distinguishing it from predictive machine learning models like multilayer perceptrons and spatial multi-criteria approaches, with its spectral formulation detailed in the methods section (Şen et al. 2020; Abu Arra et al. 2025).

Northeastern Algeria, a region critical for its economy and population, experiences rising drought frequency, with studies reporting a 20–30% rainfall decline and increased aridity (Taibi et al. 2013; Boudiaf et al. 2021; Boulmaiz and Boutaghane 2022; Berhail and Katipoğlu 2024). Regional studies using the Mann–Kendall test show varied trends: Bougara et al. (2021) reported no significant trends in the Tafna basin (1979–2011), while Choutri and Hussein (2024) detected negative trends across all timescales (1950–2020); Bessaklia et al. (2018) observed increased high precipitation events at 23 stations, yet Ziari and Medjerab (2025) noted a rainfall decrease in Annaba since June 2002 (1981–2021); Bendjema et al. (2019) identified a dry phase (1979–2001) followed by a wet phase (2002–2009) in the Mellah catchment. Although ITA has been applied to regional rainfall, its use with drought indices remains limited. FITA, as a novel modeling approach, provides a robust framework to analyze SPI, RDI, and SDI trends by integrating frequency analysis with ITA's trend detection, offering probabilistic insights into drought severity distributions. This study uses FITA and ITA to evaluate drought dynamics across 10 stations in northeastern Algeria (1975–2021), aiming to identify spatial and temporal trends and assess data homogeneity, thereby supporting integrated drought management and sustainable water resource management through connections to hydrological and ecological outcomes.

Materials and methodologies

This study analyzed long-term hydrological and meteorological data from 1975 to 2021 across multiple stations in the North-Eastern of Algeria. Monthly Precipitation, Temperature, and Flowstream data were sourced from 10 stations cover all the study area. The Frequency Innovative Trends and Statistics Analysis (FITA) was applied to assess drought trends using the Standardized Precipitation Index (SPI12), Reconnaissance Drought Index (RDI12), and Streamflow Drought Index (SDI12), calculated on a 12-month scale to capture annual drought patterns. For homogeneity assessment, Precipitation and Temperature data underwent the Levene test to evaluate variance equality across three periods (1975–1990, 1991–2005, 2006–2021), followed by the Mann–Whitney U test for pairwise distributional comparisons in inhomogeneous cases ($p \leq 0.05$). Flowstream data were analyzed using the Kruskal–Wallis test to detect overall distributional differences across the periods, with Dunn's post hoc test (Bonferroni-adjusted) applied to identify specific period pairs with significant shifts ($p \leq 0.05$).

Study area

The study area is located in northeastern Algeria, extending between longitude 6°41′ and 8°39′ E and latitude 35°12′ and 36°57′ N, covering a total area of 22,354 km^2 with a population of 5,396,900 inhabitants in 2020, distributed across eight wilayas: Annaba, El Tarf, Guelma, Skikda, Souk-Ahras, Oum-El Bouaghi, Khenchela, and Tebessa. The region's topography is characterized by the Tellian Mountains, which form a ridge along the Mediterranean Sea up to the Tunisian border (Fig. 1). The area is divided into four (4) altitude ranges along a north–south axis: the 0 to 400 m range includes the northern coastal strip of the Tell Atlas, encompassing the valleys of Oued Guebli and Oued Safsaf, the Azzaba depression, the plains of Guerbes, Annaba-Skikda, Annaba, and Tarf, and the coastal hills of El-Kala; the 400 to 800 m zone comprises the Skikda-l'Eddough Mountains, high plains of Chelghoum-Laïd, Sadrata-Taoura, Oum-El-Bouaghi, Ain-Beida, El-Madher-Chemora, Bir-El-Ater, and hills of Oued Zenati; the 800 to 1200 m range includes the high plains of Khenchela and Ain-Djasser; and the 1200 to 2200 m zone features the Aures Mountains—El-Mahmel, 2200 m—and Tebessa Mountains.

The study area, defined by a Mediterranean climate, exhibits annual precipitation ranging from 200 to 1500 mm, with a pronounced southward decline, accompanied by a warming trend of 1–2 °C per century that has exacerbated drought conditions since the 1970s, reflecting notable spatial variability. Winter months feature significant snowfall, with temperatures varying between 1 and 15 °C, whereas summer temperatures extend from 25 to 46 °C. The region is further shaped by the influence of sirocco and northwest winds, which exert distinct effects on specific sub-regions. Water resources are approximated at 308 million cubic meters per annum, highlighting the pivotal hydrological dynamics underpinning the area's environmental framework.

Dataset description for drought analysis

Data for this study consist of monthly time series of Precipitation, Temperature, and Flowstream collected from 1975 to 2021 across ten stations for Precipitation and Temperature (Annaba, Zerdaza Dam, Bekouche Lakhdar, Chafia Dam, Medjaz Amar, El-Kala, Khenchela, Oum-El Bouaghi, Souk Ahras, and Tebessa) and four stations for Flowstream (Zerdaza Dam, Bekouche Lakhdar, Chafia Dam, and Medjaz Amar). These datasets, likely sourced from the National Agency of water Resources (ANRH), were used to compute the 12-month Standardized Precipitation Index (SPI12), Reconnaissance Drought Index (RDI12), and Streamflow Drought Index (SDI12) for drought trend analysis, while also serving as the basis for homogeneity tests across the periods 1975–2021.

The study period from 1975 to 2021 was divided into three sub-periods 1975–1990, 1991–2005, and 2006–2021 to facilitate the analysis of temporal trends and homogeneity in drought indices, Precipitation, Temperature, and Flowstream data. This division was chosen to create approximately equal intervals of 15–16 years, ensuring sufficient sample sizes for robust statistical comparisons while aligning with significant climatic and anthropogenic shifts in the Mediterranean region. The 1975–1990 period serves as a baseline, reflecting a time of relatively higher precipitation and less pronounced warming in the Mediterranean, before the marked decline in rainfall observed in the region since the late 1970s (Elouissi et al. 2021; Haied et al. 2023), the 1991–2005 period coincides with increased global warming and regional water management changes; for example, dam construction in Algeria increased significantly, from 13 dams in 1962 to over 50 by the early 2000s, as a response to water scarcity (Kherbache 2020).

The 2006–2021 period reflects intensified climate variability and drought frequency, Mohammed and Al-Amin (2018) indicated that by 2020, Algeria's water availability had dropped to 430 m^3 per capita annually, falling below the World Bank's water scarcity threshold of 1000 m^3. They also projected a rainfall decrease of 16–43% rainfall reduction in northern Algeria over the twentieth century (Taibi et al. 2013), exacerbating low dam reserves throughout North Africa. This three-part framework facilitates the identification of long-term trends and possible shifts in data uniformity, aligning with the study's goal of evaluating drought patterns and ensuring data reliability over time.

Standardized Precipitation Index (SPI)

Drought poses a major natural threat, inflicting considerable socio-economic and ecological harm, contributing to about 22% of global economic losses (Malik et al. 2021). Defined by its severity, spatial coverage, duration, and timing, drought is assessed through climatic or hydrometeorological indices to support monitoring, early warning mechanisms, and impact evaluation (WMO 2016). Although drought patterns differ across regions, their analysis typically relies on meteorological station data reflecting larger areas. Various methods are available for drought monitoring, utilizing single or combined indices to improve accuracy and prediction. Among these, the Standardized Precipitation Index (SPI) is mathematically formulated as:

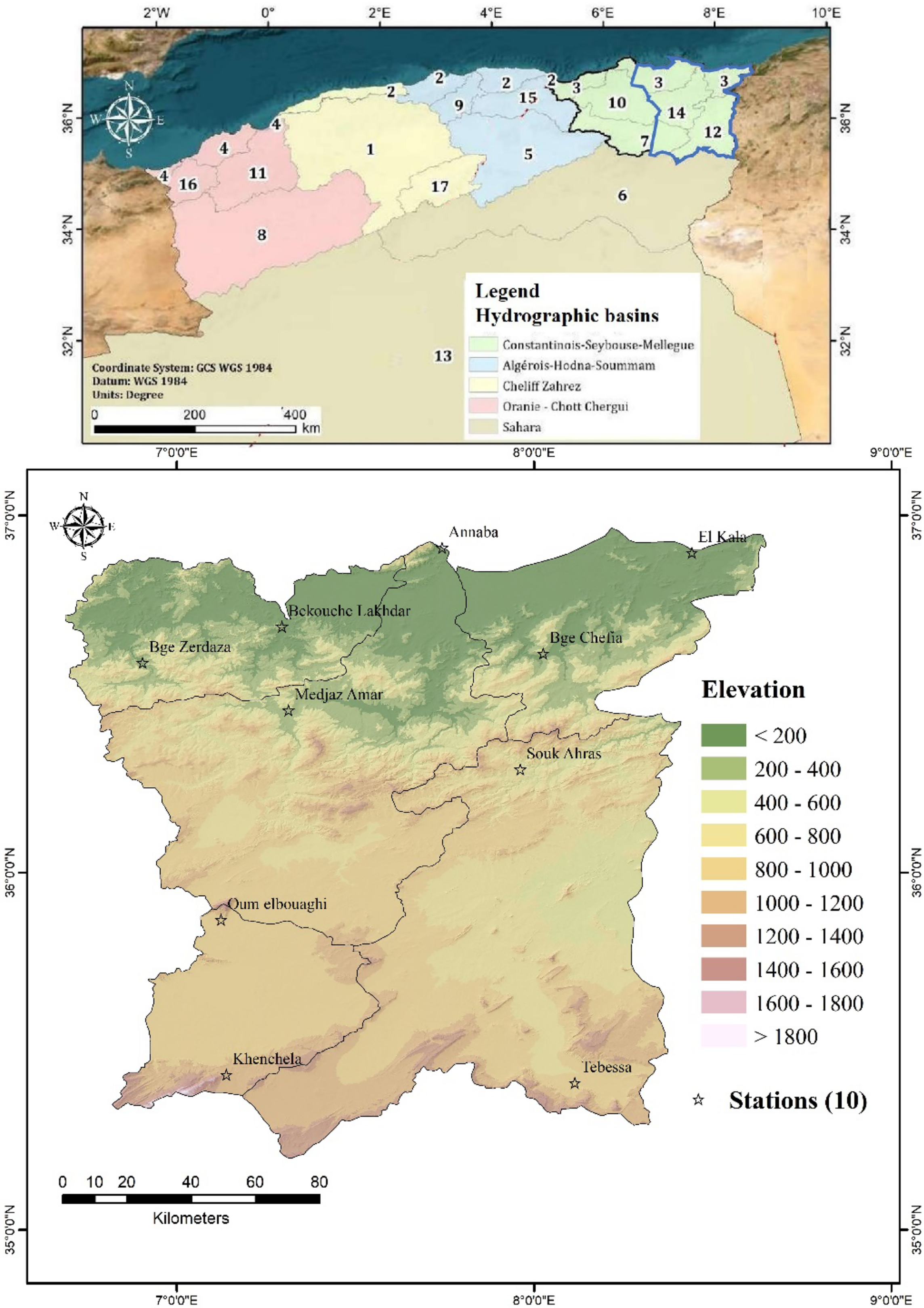

Fig. 1 Geographic situation of the study area and stations used in the study

$$SPI = \frac{\left(P_{ij} - \overline{PX}\right)}{\sigma} \quad (1)$$

where, Pij represents seasonal precipitation at the ith gauge and jth observation $\overline{P}$: denotes the long-term seasonal mean, and σ stands for the standard deviation.

The SPI effectively identifies dry and wet periods by quantifying precipitation anomalies. A drought occurs when SPI values remain below − 1 for consecutive periods and ends when they turn positive. Drought severity is classified using SPI thresholds. (Tsakiris and Vangelis 2004).

Reconnaissance Drought Index (RDI)

The Reconnaissance Drought Index (RDI) assesses drought by incorporating precipitation and potential evapotranspiration (PET) for a more precise evaluation of water deficits. Unlike traditional indices, RDI provides a comprehensive drought representation, making it effective for comparing severity across diverse climates. While RDI trends align with SPI, it is more sensitive to environmental changes, enhancing drought monitoring (Buttafuoco et al. 2016). Its universal applicability allows assessments across various climatic settings (Tigkas et al. 2015). The RDI is computed using precipitation and PET data expressed in three forms: initial value (α_k). normalized RDI (RDI_n). and standardized RDI (RDI_{st}).

The initial value α_k of RDI can be calculated for the i year on a time basis of k (months) using the following equation:

$$\propto_k^i = \frac{\sum_{j=1}^{k} P_{ij}}{\sum_{j=1}^{k} PET_{ij}} .i = 1(1)Netj = 1(1)k \quad (2)$$

where P_{ij} and PET_{ij} are the precipitation and potential evapotranspiration for month j of hydrological year i.

The values of α_k generally follow log-normal and gamma distributions across a wide range of locations and time scales, as tested. Assuming the log-normal distribution applies, the following equation can be used to calculate the standardized RDI (RDI_{st}):

$$RDI_{st}^{(i)} = \frac{y^{(i)} - \overline{y}}{\hat{\sigma}_y} \quad (3)$$

where $y^{(i)}$ is $\left(\propto_k^i\right)$, $\overline{y_k}$ is its arithmetic mean, and $\hat{\sigma}_y$ is its standard deviation.

Positive RDI_st values indicate wet periods, while negative values signify dry periods relative to the region's normal conditions. Drought severity is categorized into mild, moderate, severe, and extreme levels based on RDI thresholds.

Streamflow Drought Index (SDI)

The Streamflow Drought Index (SDI) (Nalbantis and Tsakiris 2009) extends SPI by using monthly streamflow data to assess hydrological drought. It employs normalization techniques to identify wet and dry periods while measuring drought intensity. SDI is useful for station-based drought monitoring but may not fully represent entire basins. The SDI is computed using cumulative streamflow values over specific reference periods as follows:

$$V_{i.k} = \sum_{j=1}^{3k} Q_{ij} .\text{i} = 1.2\ldots\ .\text{j} = 1.2.\ldots.12.\ \text{k} = 1.2.3.4 \quad (4)$$

where, $V_{i.k}$, is the cumulative flow of hydrological year (i) for reference period (k); $K = 1$, for October-December, $K = 2$ for October–March, $K = 3$ for October-June, and $K = 4$ for October-September.

Using the calculated cumulative streamflows, the SDI for each reference period k is determined as:

$$SDI_{i.k} = \frac{V_{i.k-\overline{Vk}}}{Sk} .\text{i} = 1.2.....\ \text{K} = 1.2.3.4 \quad (5)$$

where, V_k and S_k are the mean and standard deviation respectively of cumulative flows for reference period k calculated over a long period.

The SDI classification follows a structure similar to meteorological drought indices like SPI, defining five levels of hydrological drought severity. This index is widely used to evaluate long-term water availability assess watershed response to drought, and support water resource management strategies.

Innovative trend analysis (ITA)

Introduced by Şen (2012), is a nonparametric method for detecting monotonic trends (increasing or decreasing) in hydroclimatic time series (e.g., precipitation, SPI). It compares two equal halves of a time series on a scatter plot, avoiding assumptions like normality or stationarity required by methods like Mann–Kendall (Mann 1945; Kendall 1975).

ITA divides a time series $X = \left(x_1, x_2, \ldots\ldots, x_{n/2}\right)$ into equal sub-series:

$$X_1 = \left(x_1, x_2, \ldots\ldots, x_{n/2}\right), X_2 = \left(x_{(n/2)+1}, \ldots\ldots, x_n\right)$$

Each sub-series is sorted in ascending order and plotted against each other as a scatterplot:

$$x_i^{(1)} vs x_i^{(2)} for i = 1, \ldots\ldots., n/2 \quad (6)$$

A 45° line (the identity line) is drawn. The location of the points relative to this line indicates the trend:

- Points above the line → increasing trend
- Points below the line → decreasing trend
- Points around the line → no trend

The ITA slope can be estimated by simple linear regression between the ordered sub-series:

$$Slope_{ITA} = \frac{\sum_{i=1}^{n/2}\left(x_i^{(2)} - \overline{x}^{(2)}\right)\left(x_i^{(1)} - \overline{x}^{(1)}\right)}{\sum_{i=1}^{n/2}\left(x_i^{(1)} - \overline{x}^{(1)}\right)^2} \tag{7}$$

where $\overline{x}^{(1)}$ and $\overline{x}^{(2)}$ are the means of each sub-series (Fig. 2).

FITA analysis

Frequency analysis (Eq. 8) quantifies the occurrence, intensity, and persistence of drought classifications, aiding in the evaluation of drought patterns and severities. The Frequency Innovative Trends and Statistics Analysis (FITA) is a novel methodology designed to detect trends in hydrometeorological time series by emphasizing frequency-based patterns over time (Abu Arra et al. 2024). FITA is inspired by methods like Şen's Innovative Trend Analysis (ITA), which plots time series subsections to visually detect trends without strict statistical assumptions. FITA's frequency focus suggests an additional layer of spectral analysis, which is common in climate studies to identify cycles. It proposes an additional to the ITA graph, representing the frequency of each drought classification. Drought classifications can include categories such as: normal, moderate drought, severe drought, and extreme drought as reported in Table 1.

$$Frequency = \frac{Numberofmonthsineachclassification}{Totalnumberofmonths} \times 100\% \tag{8}$$

FITA likely employs frequency-domain techniques, such as spectral analysis or wavelet transforms (Rezaiy and Shabri 2025), to identify periodicities and trends in drought occurrences, offering an advantage over traditional methods like Mann–Kendall by not requiring restrictive assumptions (data independence or normality). The methodology involves: (1)

Table 1 Drought classification according to McKee et al. (Abu Arra et al. 2025)

(Drought Index value_DI)	Drought classification	Probability (%)
2.00 ≤ DI	Extreme wet (EW)	2.3%
1.50 ≤ DI < 2.00	Severe wet (SW)	4.4%
1.00 ≤ DI < 1.50	Moderate wet (MW)	9.2%
1.00 < DI < 1.00	Normal (N)	68.2%
1.50 ≤ DI ≤ − 1.00	Moderate drought (MD)	9.2%
2.00 < DI ≤ 1.50	Severe drought (SD)	4.4%
2.00 ≥ DI	Extreme drought (ED)	2.3%

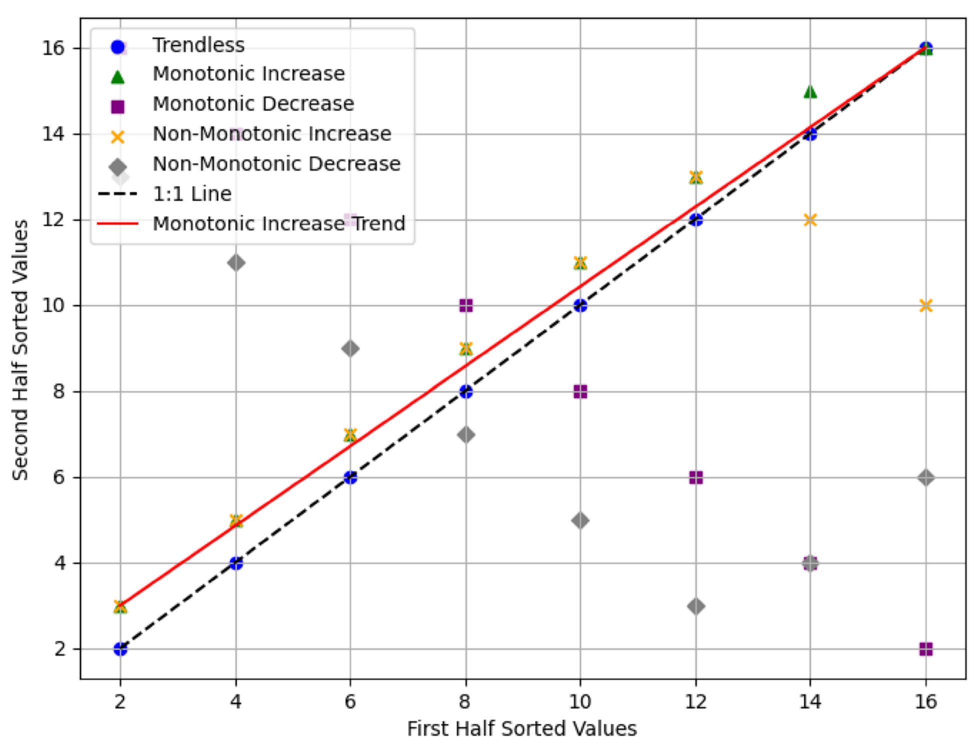

Fig. 2 Scatter Plot Representation of Innovative Trend Analysis (ITA) Trend Types (Dabanlı et al. 2016)

transforming the time series of each drought index into the frequency domain to detect dominant cycles, (2) analyzing trends in the frequency of drought events across the study period, and (3) comparing trends across the three defined periods (1975–1990, 1991–2005, 2006–2021) to assess temporal shifts. This approach enables a nuanced understanding of drought dynamics, revealing both short-term fluctuations and long-term trends. Figure 3 illustrates the operational framework of the Frequency Innovative Trend Analysis (FITA) method.

Homogeneity tests

Detecting trends and ensuring data homogeneity in long-term hydrological and meteorological records pose significant challenges for drought monitoring and climate analysis. Over the 1975–2021 period, datasets like Precipitation, Temperature, and Flowstream often exhibit non-stationarities due to climate variability, human interventions (dams, land use changes), and data inconsistencies (station relocations, instrument upgrades).

This section evaluates the homogeneity of Precipitation, Temperature, and Flowstream data across three periods (1975–1990, 1991–2005, 2006–2021) using robust statistical tests. The Levene and Mann–Whitney U tests were applied to Precipitation and Temperature, while the Kruskal–Wallis and Dunn's post hoc tests were used for Flowstream to identify significant temporal shifts.

Levene's test

Levene's test, a statistical method, evaluates the homogeneity of variances among multiple groups by determining if the variances of various samples are equal, a critical assumption for parametric tests such as ANOVA. Notably, this test is independent of sample variances, making it relatively insensitive to outliers (Levene 1960).

For a dataset divided into k groups, each with ni observations, the test statistic is computed as:

$$W = \frac{(N-K)}{K-1} \times \frac{\sum_{i=1}^{k} n_i \left(Z_i - Z_{..}\right)^2}{\sum_{i=1}^{k} \sum_{j=1}^{n_i} \left(Z_{ij} - Z_i\right)^2} \tag{9}$$

where, N, is the total number of observations across all groups; k, is the number of groups; $Z_{ij} = \left|X_{ij} - \dot{X}_i\right|$, is the absolute deviation from the group median (for a robust version) or mean (original version); Z_i, is the mean of Z_{ij} within group i; $Z_{..}$, is the overall mean of Z_{ij} across all groups.

If the test statistic W is significant (p value < chosen alpha level, typically 0.05), the assumption of equal variances is violated.

Mann Whitney U test

The Mann–Whitney U test, also known as the Wilcoxon rank-sum test, serves as a nonparametric counterpart to the student's t-test, comparing the means of two independent groups without assuming a normal distribution of the data (Hart 2001; Sheskin 2007). For two independent samples, X (with size n1) and Y (with size n2), the U statistic is calculated as follows:

$$U_1 = n_1 n_2 + \frac{n_1\left(n_1 + 1\right)}{2} - R_1 \tag{10}$$

where, R_1, is the sum of the ranks assigned to the observations in sample X.

A second U statistic is calculated similarly for sample Y:

$$U_2 = n_1 n_2 + \frac{n_2\left(n_2 + 1\right)}{2} - R_2 \tag{11}$$

The smaller of U_1 and U_2 is typically used as the test statistic.

The p value linked to the U statistic reflects the likelihood of obtaining the observed result if the null hypothesis—that both groups share the same distribution—holds true. A low p value ($p < 0.05$) indicates strong evidence to reject the null hypothesis, pointing to a notable difference between the groups (Sheskin 2007; Krzywinski and Altman 2014).

Kruskal–Wallis and Dunn's post hoc tests

The Kruskal–Wallis test is a non-parametric statistical method used to compare the distributions of three or more independent groups when the data do not meet the assumptions of normality required for a one-way ANOVA. Proposed by Kruskal and Wallis (1952), the test extends the Mann–Whitney U test to multiple groups, evaluating the null hypothesis that all groups have identical distributions against the alternative that at least one group differs. It operates by ranking all observations across groups, calculating the mean rank for each group, and computing a test statistic (H) based on the differences in mean ranks, adjusted for sample sizes. The H statistic follows a chi-square distribution, and a p value ≤ 0.05 typically indicates significant differences among groups. When the Kruskal–Wallis test rejects the null hypothesis, Dunn's post hoc test is often applied to identify which specific pairs of groups differ. Introduced by Dunn (1964), this test performs pairwise comparisons using rank sums, adjusting for multiple comparisons to control the family-wise error rate, commonly with the Bonferroni correction (Bewick et al. 2004; Kim 2014).

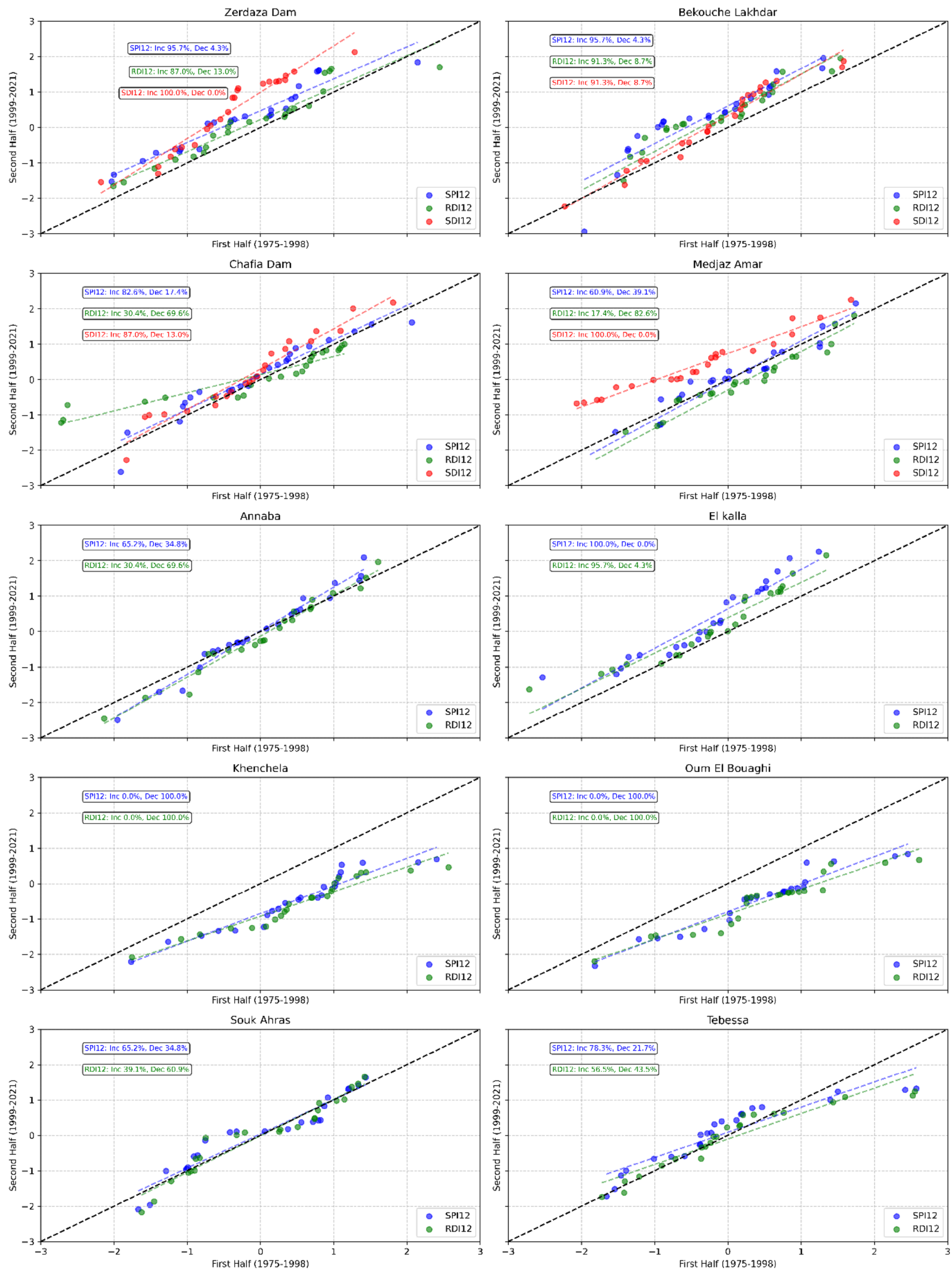

Fig. 3 Frequency and Innovative Trend Analysis (FITA and ITA) of SPI12, RDI12, and SDI12 for 10 Stations in Northeastern Algeria (1975–2021)

Results

FITA and temporal variability of drought indices

The FITA analysis of SPI12, RDI12, and SDI12 from 1975 to 2021 shows varying drought trends across northeastern Algeria. Figure 3 reveals a downward trend in sorted DI values from 1975–1998 to 1999–2021, with points below the 1:1 line. Inland stations like Khenchela and Oum El Bouaghi report 100% decreasing SPI12, while coastal stations like El Kalla show 100% increasing SPI12 and Zerdaza Dam 95.65% increasing SPI12. Medjaz Amar exhibits 100% increasing SDI12 and 82.61% decreasing RDI12.

Boxplots in Fig. 4 compare precipitation, temperature, and streamflow variations over the three defined time periods.

The boxplots reveal distinct patterns Precipitation exhibits high variability across all stations (Annaba, Zerdaza Dam, Khenchela), with medians generally decreasing from 1975–1990 to 2006–2021, particularly at stations like Souk Ahras and Oum-El Bouaghi, where the 2006–2021 period shows a tighter interquartile range and more frequent low outliers, indicating reduced rainfall and potential drought intensification.

Temperature boxplots show a consistent upward shift in medians across all stations (Chafia Dam, Medjaz Amar), with the 2006–2021 period displaying higher medians (for example, 20 °C at Annaba) compared to 1975–1990 (18 °C), alongside increased variability and high outliers, reflecting warming trends that exacerbate drought conditions.

Flowstream data indicate significant variability, especially at Zerdaza Dam and Medjaz Amar, where medians drop sharply in 1991–2005 and 2006–2021 compared to 1975–1990, with numerous low outliers in the latter period suggesting reduced streamflow and heightened drought severity.

Homogeneity analysis

Homogeneity tests were conducted to assess the consistency of Precipitation, Temperature, and Flowstream data across the three periods (1975–1990, 1991–2005, 2006–2021) for all stations in northeastern Algeria, using a significance threshold of $p \leq 0.05$ as reported in Table 2.

For Precipitation, the Levene test revealed that most stations exhibit homogeneous variance (Annaba, $p = 0.7145$; Zerdaza Dam, $p = 0.252$), indicating stable data consistency over time. However, Khenchela ($p = 0.0005$), Oum El Bouaghi ($p = 0.0$), and Souk Ahras ($p = 0.0045$) were found to be inhomogeneous, suggesting significant variance changes.

Subsequent Mann–Whitney U tests on these stations showed no significant distributional differences between periods (Khenchela: $p = 0.9408$ for 1975–1990 vs 1991–2005), indicating that the inhomogeneity is primarily due to variance shifts rather than changes in the overall distribution.

For Temperature, the Levene test indicated homogeneity across most stations (Annaba, $p = 0.3642$; Medjaz Amar, $p = 0.8382$), except for Chafia Dam ($p = 0.0471$), which was inhomogeneous. However, Mann–Whitney U tests for Chafia Dam revealed no significant distributional differences ($p = 0.2653$ for 1975–1990 vs 1991–2005; $p = 0.1651$ for 1991–2005 vs 2006–2021), suggesting that the inhomogeneity is also driven by variance changes rather than distributional shifts.

In contrast, Flowstream data exhibited significant inhomogeneity across all stations, as determined by the Kruskal–Wallis test ($p \leq 0.0103$ for Zerdaza Dam, Bekouche

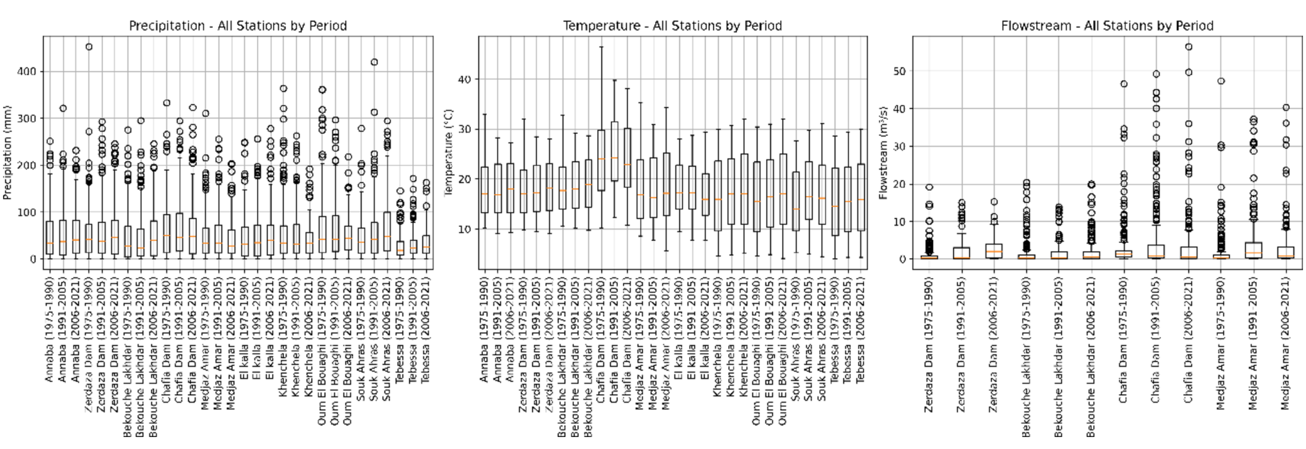

Fig. 4 Temporal Variability of Precipitation, Temperature, and Flowstream Across Stations in Northeastern Algeria (1975–2021)

Table 2 Homogeneity test results for precipitation, temperature, and flowstream across stations in Northeastern Algeria (1975–2021)

Variable	Station	Levene *p* value	Homogeneity	MW *p* value (1975–1990 vs 1991–2005)	MW *p* value (1991–2005 vs 2006–2021)
Precipitation	Annaba	0.7145	Homogeneous	–	–
Precipitation	Zerdaza Dam	0.2520	Homogeneous	–	–
Precipitation	Bekouche Lakhdar	0.3364	Homogeneous	–	–
Precipitation	Chafia Dam	0.8922	Homogeneous	–	–
Precipitation	Medjaz Amar	0.6600	Homogeneous	–	–
Precipitation	El kalla	0.4139	Homogeneous	–	–
Precipitation	Khenchela	0.0005	Inhomogeneous	0.9408	0.4044
Precipitation	Oum El Bouaghi	0.0000	Inhomogeneous	0.9329	0.5827
Precipitation	Souk Ahras	0.0045	Inhomogeneous	0.3074	0.1429
Precipitation	Tebessa	0.1018	Homogeneous	–	–
Temperature	Annaba	0.3642	Homogeneous	–	–
Temperature	Zerdaza Dam	0.5081	Homogeneous	–	–
Temperature	Bekouche Lakhdar	0.5079	Homogeneous	–	–
Temperature	Chafia Dam	0.0471	Inhomogeneous	0.2653	0.1651
Temperature	Medjaz Amar	0.8382	Homogeneous	–	–
Temperature	El kalla	0.5966	Homogeneous	–	–
Temperature	Khenchela	0.7394	Homogeneous	–	–
Temperature	Oum El Bouaghi	0.8502	Homogeneous	–	–
Temperature	Souk Ahras	0.6204	Homogeneous	–	–
Temperature	Tebessa	0.7416	Homogeneous	–	–
Flowstream	Zerdaza Dam	0.0000	Inhomogeneous	0.0025	0.0007
Flowstream	Bekouche Lakhdar	0.7456	Homogeneous	–	–
Flowstream	Chafia Dam	0.1222	Homogeneous	–	–
Flowstream	Medjaz Amar	0.0255	Inhomogeneous	0.0000	0.0259

Lakhdar, Chafia Dam, and Medjaz Amar), indicating substantial distributional differences over time.

Frome Table 3, Dunn's post hoc tests with Bonferroni correction further highlighted specific period shifts: Zerdaza Dam and Medjaz Amar showed near-significant or significant differences across all period pairs (Zerdaza Dam: $p = 0.0527$ for 1975–1990 vs 1991–2005, $p = 0.05$ for 1975–1990 vs 2006–2021; Medjaz Amar: $p = 0.05$ for 1975–1990 vs 1991–2005, $p = 0.0503$ for 1975–1990 vs 2006–2021), suggesting consistent temporal shifts in flowstream behavior. Bekouche Lakhdar and Chafia Dam exhibited significant shifts primarily between 1975–1990 and 2006–2021 (Bekouche Lakhdar: $p = 0.05113$; Chafia Dam: $p = 0.063$), with less pronounced differences in other pairs (Bekouche Lakhdar: $p = 1.0$ for 1975–1990 vs 1991–2005; Chafia Dam: $p = 0.438$ for 1991–2005 vs 2006–2021).

These Flowstream results are visualized in Fig. 5, a heatmap displaying the Kruskal–Wallis and Dunn's post hoc *p* values, where lower *p* values (red shades) indicate significant differences, particularly for Zerdaza Dam and Medjaz Amar across all periods, and for Bekouche Lakhdar and Chafia Dam between the earliest and latest periods. These findings underscore the varying degrees of data consistency

Table 3 Kruskal–Wallis and Dunn's post hoc test results for flowstream homogeneity across stations in northeastern Algeria (1975–2021)

Variable	Station	Kruskal–Wallis *p* value	Homogeneity	Post hoc (1975–1990 vs 1991–2005)	Post hoc (1975–1990 vs 2006–2021)	Post hoc (1991–2005 vs 2006–2021)
Flowstream	Zerdaza Dam	0.0000	Inhomogeneous	0.0527	0.05000	0.0507
Flowstream	Bekouche Lakhdar	0.0103	Inhomogeneous	1.0000	0.05113	0.0880
Flowstream	Chafia Dam	0.0088	Inhomogeneous	0.3304	0.063	0.4380
Flowstream	Medjaz Amar	0.0000	Inhomogeneous	0.05000	0.0503	0.0817

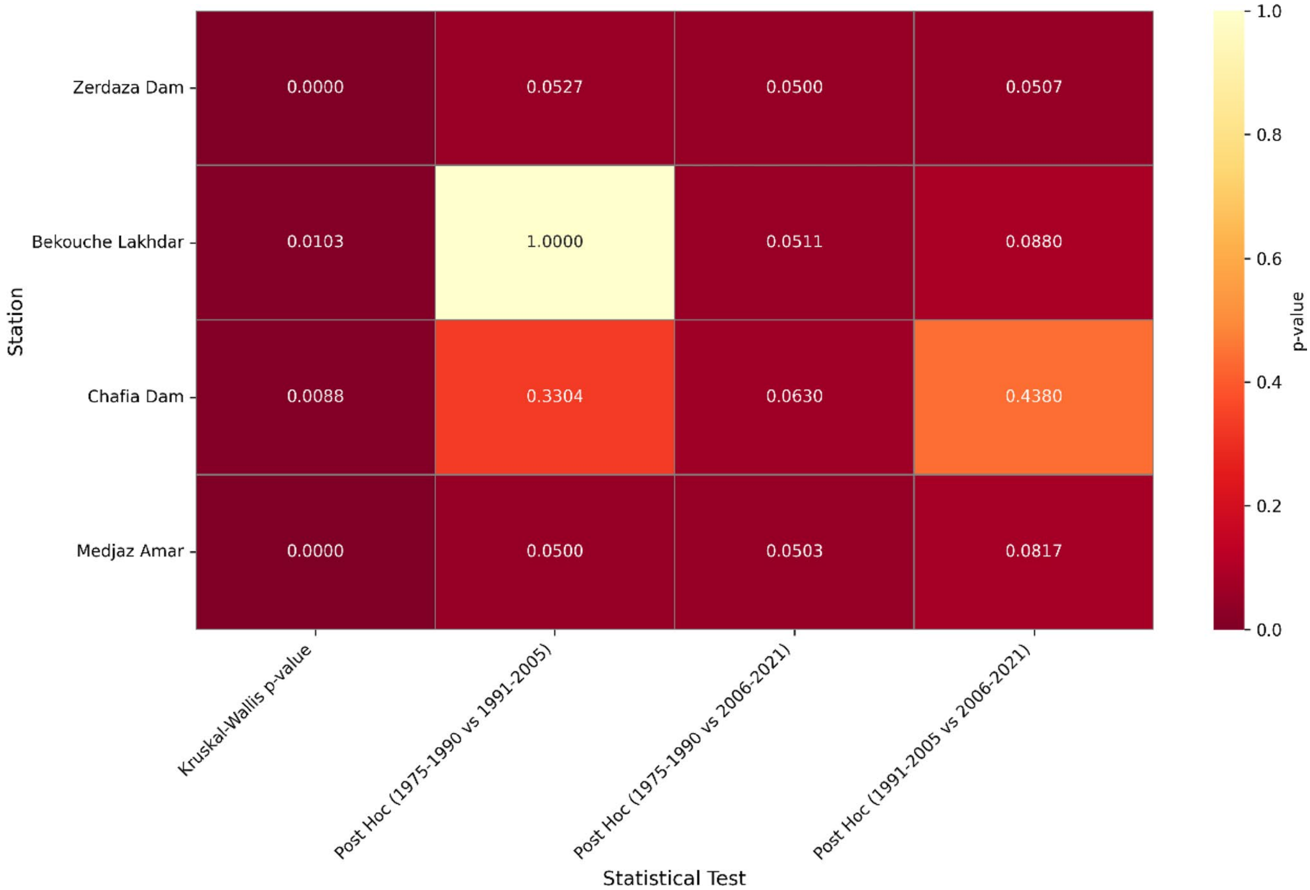

Fig. 5 Flowstream homogeneity: Kruskal-Walis and Dunn's Post Hoc *p* values

across the parameters, with Flowstream showing the most pronounced temporal instability.

Trend frequencies and ITA slopes

Table 4 lists FITA derived trend frequencies and ITA slopes. Khenchela shows 100% decreasing SPI12 (ITA slope: −0.846) and RDI12 (ITA slope: −0.792). El Kalla exhibits 100% increasing SPI12 (ITA slope: 1.160) and 95.65% increasing RDI12. Medjaz Amar has 100% increasing SDI12 (ITA slope: 0.797) and 82.61% decreasing RDI12 (ITA slope: −1.294). Zerdaza Dam reports 95.65% increasing SPI12 (ITA slope: 0.596) and 86.96% increasing RDI12.

Discussion

The results of this paper all align with the observed patterns of drought across northeastern Algeria from 1975 to 2021, as analyzed through the methodologies outlined. Inland stations such as Khenchela (100% decreasing SPI12, ITA slope: −0.846) and Oum El Bouaghi (100% decreasing SPI12, ITA slope: −0.864) exhibit persistent meteorological drought, corroborated by declining Precipitation medians shown in Fig. 4. In contrast, stations like El Kalla (100% increasing SPI12, ITA slope: 1.160) and Zerdaza Dam (95.65% increasing SPI12, ITA slope: 0.596) show wetter conditions, likely influenced by proximity to the Mediterranean Sea, which may mitigate regional precipitation declines. At Medjaz Amar, mixed trends (100% increasing SDI12, ITA slope: 0.797; 82.61% decreasing RDI12, ITA slope: −1.294) indicate streamflow recovery alongside worsening agricultural drought, a pattern effectively captured by the ITA-FITA methodology's ability to detect spatial and sectoral variability, as depicted in Fig. 3.

The homogeneity analysis (Tables 2 and 3) supports the observed significant Flowstream inhomogeneity (Kruskal–Wallis $p \leq 0.0103$), with notable shifts at Zerdaza Dam ($p = 0.05$ for 1975–1990 vs. 2006–2021) and Medjaz Amar, attributable to dam operations and a documented 16–43% rainfall decline (Taibi et al. 2013). Precipitation and Temperature data remain largely homogeneous (e.g., Annaba, $p = 0.7145$), ensuring the reliability of SPI12 and RDI12 trends, though Khenchela's variance shift ($p = 0.0005$) aligns with its sustained drought conditions, reinforcing the analysis's validity.

Table 4 FITA-derived trend frequencies for SPI12, RDI12, and SDI12 across stations in northeastern Algeria (1975–2021)

Station	Index	Increasing (%)	Decreasing (%)	No trend (%)	Years
Zerdaza Dam	SPI12	95,65	4,35	0	1975–2021
Zerdaza Dam	RDI12	86,96	13,04	0	1975–2021
Bekouche Lakhdar	SPI12	95,65	4,35	0	1975–2021
Bekouche Lakhdar	RDI12	91,3	8,7	0	1975–2021
Bekouche Lakhdar	SDI12	91,3	8,7	0	1975–2021
Chafia Dam	SPI12	82,61	17,39	0	1975–2021
Chafia Dam	RDI12	30,43	69,57	0	1975–2021
Chafia Dam	SDI12	86,96	13,04	0	1975–2021
Medjaz Amar	SPI12	60,87	39,13	0	1975–2021
Medjaz Amar	RDI12	17,39	82,61	0	1975–2021
Medjaz Amar	SDI12	100	0	0	1975–2021
Annaba	SPI12	65,22	34,78	0	1975–2021
Annaba	RDI12	30,43	69,57	0	1975–2021
El kalla	SPI12	100	0	0	1975–2021
El kalla	RDI12	95,65	4,35	0	1975–2021
Khenchela	SPI12	0	100	0	1975–2021
Khenchela	RDI12	0	100	0	1975–2021
Oum El Bouaghi	SPI12	0	100	0	1975–2021
Oum El Bouaghi	RDI12	0	100	0	1975–2021
Souk Ahras	SPI12	65,22	34,78	0	1975–2021
Souk Ahras	RDI12	39,13	60,87	0	1975–2021
Tebessa	SPI12	78,26	21,74	0	1975–2021
Tebessa	RDI12	56,52	43,48	0	1975–2021

Hydrological changes, visualized in the heatmap (Fig. 5), point to significant impacts from anthropogenic activities, particularly dam operations at Zerdaza and Chafia Dams, which regulate flow for irrigation and water supply. Climatic factors, including a rainfall reduction in northern Algeria and increased evaporation due to rising temperatures (Fig. 2: medians of 20 °C in 2006–2021 vs. 18 °C in 1975–1990), further diminish natural streamflow. El Kalla and Zerdaza Dam's positive SPI12 trends suggest wetter conditions, possibly buffered by Mediterranean influences, while Khenchela and Oum El Bouaghi's negative SPI12 trends (slopes of − 0.846 and − 0.864) indicate prolonged moderate to severe drought (SPI12 likely below − 1), consistent with a 20–30% rainfall decrease over the twentieth century (Mrad et al. 2018). Figure 4's boxplots, showing Khenchela's Precipitation medians dropping with frequent low outliers near zero, support this pattern.

RDI12 trends underscore temperature's aggravating role. At Chafia Dam, a 69.57% decrease in RDI12 (ITA slope: − 0.708), despite an 82.61% increase in SPI12 (ITA slope: 0.947), highlights how elevated temperatures (medians rising from 18 to 20 °C) boost evapotranspiration, intensifying agricultural drought. Similarly, Medjaz Amar's 82.61% RDI12 decrease (ITA slope: − 1.294) contrasts with a 100% SDI12 increase (ITA slope: 0.797), indicating that streamflow improvements do not offset agricultural water deficits. These ITA slopes-negative for Khenchela (− 0.846 for SPI12, − 0.792 for RDI12) and positive for Medjaz Amar's SDI12 (0.797)—quantify the divergent hydrological and agricultural trends with precision.

These patterns align with regional climate dynamics, as Essa et al. (2023) note a pronounced drought intensification in the southern Mediterranean, particularly in North Africa. Mrad et al. (2018) further confirm a north-to-south rainfall gradient in Algeria, amplifying aridity concerns. Anthropogenic influences, including dam operations and land use changes, significantly alter the hydrological balance, as evidenced by Hassini et al. (2011), Meddi (2013), Balah and Amarchi (2016), and Kourat and Medjerab (2016). However, the increasing trends at El Kalla and Zerdaza Dam suggest localized resilience, potentially due to microclimatic factors or effective water management, warranting further investigation.

The environmental consequences are significant. At Khenchela, the 100% decreasing SPI12 trend reduces groundwater recharge, threatening the Chott Melghir wetland—a critical biodiversity hotspot (AMARD 2014)—and heightens desertification risks, with Denidina et al. (2020) reporting vegetation cover loss in southern Algerian steppes. Haied et al. (2023) document similar drought severity in semi-arid Algeria, where groundwater declines (e.g., 41% over 17 years in Morocco's Haouz Plain) stress ecosystems.

Wetter conditions at Zerdaza Dam, reflected by its SPI12 increase, may lead to soil erosion and sedimentation, reducing reservoir capacity and disrupting aquatic ecosystems, as indicated by Fig. 4's Flowstream decline. Rising temperatures exacerbate these issues, particularly at Medjaz Amar, where agricultural drought intensifies despite streamflow gains.

To address these challenges, the recommendation for integrated management strategies, such as rainwater harvesting (Guebail et al. 2017), is well-supported by the ITA-FITA findings of spatial variability. Implementing early warning systems based on SPI12 and SDI12 can enhance resilience, mitigating drought impacts on water resources, ecosystems, and land use in this semi-arid region. In summary, the ITA-FITA methodology, validated by homogeneity tests (Tables 2 and 3) and temporal data (Fig. 4), provides a solid foundation for understanding these trends and guiding adaptive strategies.

Conclusion

In summary, this investigation underscores the value of evaluating drought patterns in northeastern Algeria (1975–2021) through the Frequency Innovative Trends and Statistics Analysis (FITA) and Innovative Trend Analysis (ITA) approaches, implemented across ten stations using SPI12, RDI12, and SDI12 indices, uncovering significant ecological consequences. These techniques blend frequency assessments of drought intensities within the time series, facilitating a detailed examination of how drought behaviors shift over time and delivering a comprehensive view of diverse drought magnitudes.

The principal findings are outlined as follows:

- Integrating frequency and drought categorization enhances the analysis of drought trends beyond mere rises or falls, enabling a precise study of meteorological, agricultural, and hydrological drought variations.
- The FITA approach successfully identifies both steady and fluctuating trends in drought frequency throughout the study duration.
- The drought classification was enriched with extreme wet and dry categories, expanding on established models, to more effectively reflect the range of drought and wet occurrences.
- At Khenchela, FITA results indicated a 100% decreasing SPI12 trend (ITA slope: -0.846), signaling ongoing meteorological drought, whereas El Kalla displayed a 100% increasing SPI12 trend (ITA slope: 1.160), suggesting wetter conditions.
- At Medjaz Amar, FITA highlighted mixed patterns with a 100% increasing SDI12 (ITA slope: 0.797) and an 82.61% decreasing RDI12 (ITA slope: -1.294), pointing to streamflow improvement alongside worsening agricultural drought, driven by elevated temperatures (medians: 20 °C in 2006–2021 vs. 18 °C in 1975–1990, Fig. 4).
- Homogeneity assessment revealed notable Flowstream inconsistency (Kruskal–Wallis $p \leq 0.0103$) at Zerdaza Dam ($p = 0.0500$ for 1975–1990 vs. 2006–2021) and Medjaz Amar, likely due to dam activities and reduced rainfall, while Precipitation and Temperature were largely consistent (e.g., Annaba: $p = 0.7145$), though Khenchela exhibited variance shifts ($p = 0.0005$).

These patterns highlight critical ecological effects, including diminished groundwater replenishment at Khenchela endangering wetlands like Chott Melghir (AMARD 2014), heightened desertification risks with vegetation decline in southern steppes (Denidina et al. 2020), and potential sedimentation at Zerdaza Dam affecting aquatic habitats. The results advocate for holistic management approaches, such as rainwater collection (Guebail et al. 2017), and the use of these findings in early warning systems to strengthen environmental adaptability against growing drought issues in the Mediterranean region.

Author contributions AA: Conceptualization, methodology, data collection, formal analysis, writing—original draft preparation. LZ: Methodology, software, validation, writing—review and editing. MC: Data curation, visualization, writing—review and editing. HA: Conceptualization, methodology, data collection, formal analysis, writing—original draft preparation. FL Methodology, formal analysis of the revision part. All authors read and approved the final manuscript.

Funding The authors declare that no funds, grants, or other support were received during the preparation of this manuscript.

Data availability No datasets were generated or analysed during the current study.

Declarations

Competing interests The authors have no relevant financial or non-financial interests to disclose.

References

Abu Arra A, Alashan S, Şişman E (2024) Trends of meteorological and hydrological droughts and associated parameters using innovative approaches. J Hydrol 640:131661. https://doi.org/10.1016/j.jhydrol.2024.131661

Abu Arra A, Alashan S, Şişman E (2025) Advancing innovative trend analysis for drought trends: incorporating drought classification frequencies for comprehensive insights. Nat Hazards. https://doi.org/10.1007/s11069-025-07119-0

Algerian Ministry of Agriculture and Rural Development (2014) Drought management strategy in Algeria. Regional Workshop for the Near East and North Africa, Cairo, Egypt, 17–20 November 2014

Alkubaisi H, Danandeh Mehr A, Khan MMH et al (2025) Drought modelling and forecasting using shallow and deep machine learning techniques. Model Earth Syst Environ 11:41. https://doi.org/10.1007/s40808-024-02268-w

Balah B, Amarchi H (2016) Variabilité des séries pluviométriques du bassin versant de la Seybouse du Nord Est-Algérien. Rev Sci Technol Synth 32:86–97

Bendjema L, Baba-Hamed K, Bouanani A (2019) Characterization of the climatic drought indices application to the Mellah catchment, North-East of Algeria. J Water Land Dev 43:28–40. https://doi.org/10.2478/jwld-2019-0060

Berhail S, Katipoğlu OM (2024) Exploring hydrological and meteorological drought trends in Northeast Algeria: implications for water resource management. Theor Appl Climatol 155:9689–9712. https://doi.org/10.1007/s00704-024-05207-y

Bessaklia H, Ghenim AN, Megnounif A, Martín Vide J (2018) Spatial variability of concentration and aggressiveness of precipitation in North-East of Algeria. J Water Land Dev 36:3–15

Bewick V, Cheek L, Ball J (2004) Statistics review 10: further nonparametric methods. Crit Care 8:196–199. https://doi.org/10.1186/cc2857

Boudiaf B, Şen Z, Boutaghane H (2021) Climate change impact on rainfall in north-eastern Algeria using innovative trend analyses (ITA). Arab J Geosci 14:511. https://doi.org/10.1007/s12517-021-06644-z

Bougara H, Baba-Hamed K, Borgemeister C, Tischbein B, Kumar N (2021) A comparative assessment of meteorological drought in the Tafna basin, Northwestern Algeria. J Water Land Dev 51:78–93

Boulmaiz T, Boutaghane H (2022) Innovative trend analysis of daily and extremes of rainfall in North-Eastern Algeria. Int J Hydrol Sci Technol 14(2):140–153

Buttafuoco G, Caloiero T, Guagliardi I, Ricca N (2016) Drought assessment using the reconnaissance drought index (RDI) in a southern Italy region. In: Proceedings of the 6th IMEKO TC19 symposium on environmental instrumentation and measurements, Reggio Calabria, Italy, pp 24–25

Cancelliere A, Mauro GD, Bonaccorso B, Rossi G (2007) Drought forecasting using the standardized precipitation index. Water Resour Manage 21:801–819. https://doi.org/10.1007/s11269-006-9062-y

Choutri I, Hussien A (2024) Exploratory analysis of Algeria meteorological drought using SPI and SPEI. Open Access Libr J 11:1–25. https://doi.org/10.4236/oalib.1111897

Dabanlı İ, Şen Z, Yeleğen MÖ, Şişman E, Selek B, Güçlü YS (2016) Trend assessment by the innovative-Şen method. Water Resour Manage 30:5193–5203

Denidina B, Medjerab A, Mega N (2020) Characterization of drought events in south Oran and south Algiers steppes in Algeria. Int J Ecol Dev 35(1)

Djebou DCS (2017) Bridging drought and climate aridity. J Arid Environ 144:170–180. https://doi.org/10.1016/j.jaridenv.2017.05.002

Dunn OJ (1964) Multiple comparisons using rank sums. Technometrics 6:241–252. https://doi.org/10.1080/00401706.1964.10490181

Elouissi A, Benzater B, Dabanli I, Habi M, Harizia A, Hamimed A (2021) Drought investigation and trend assessment in Macta watershed (Algeria) by SPI and ITA methodology. Arab J Geosci 14:1329

Essa YH, Hirschi M, Thiery W et al (2023) Drought characteristics in Mediterranean under future climate change. NPJ Clim Atmos Sci 6:133. https://doi.org/10.1038/s41612-023-00458-4

Guebail A, Zeghadnia L, Djebbar Y, Bouranene S (2017) Rainwater harvesting in Algeria: utilization and assessment of the physicochemical quality Case study of Souk-Ahras region. Rev Cour Savr 23:85–94

Habibi B, Meddi M, Abdelkader M (2024) The frequency distribution and stochastic analysis of the hydrological drought in Northern Algeria. Ital J Agrometeorol. https://doi.org/10.36253/ijam-1730

Haied N, Foufou A, Khadri S, Boussaid A, Azlaoui M, Bougherira N (2023) Spatial and temporal assessment of drought hazard, vulnerability and risk in three different climatic zones in Algeria using two commonly used meteorological indices. Sustainability 15:7803. https://doi.org/10.3390/su15107803

Hakam O, Baali A, Belhaj Ali A (2023) Modeling drought-related yield losses using new geospatial technologies and machine learning approaches: case of the Gharb plain, North-West Morocco. Model Earth Syst Environ 9:647–667. https://doi.org/10.1007/s40808-022-01523-2

Hart A (2001) Mann-Whitney test is not just a test of medians: differences in spread can be important. BMJ 323(7309):391–393

Hassanein MK, Essa A, Khalil Y (2013) Assessment of drought impact in Africa using standard precipitation evapotranspiration index. Nat Sci 11:75–81. https://doi.org/10.1017/CBO9781107415324.004

Hassini N, Abderrahmani B, Dobbi A (2011) Trends of precipitation and drought on the Algerian littoral: impact on the water reserves. Int J Water Resour Arid Environ 1(4):271–275

Hayes M, Svoboda M, Wall N, Widhalm M (2011) The Lincoln declaration on drought indices: universal meteorological drought index recommended. Bull Am Meteorol Soc 92:485–488

Ihinegbu C, Ogunwumi T (2022) Multi-criteria modelling of drought: a study of Brandenburg Federal State, Germany. Model Earth Syst Environ 8:2035–2049. https://doi.org/10.1007/s40808-021-01197-2

IPCC (2019) Impacts of 1.5 °C of global warming on natural and human systems. https://www.ipcc.ch/site/assets/uploads/sites/2/2019/02/SR15_Chapter3_Low_Res.pdf

Jahangir MH, Zarfeshani A, Danehkar S (2024) Numerical comparison of streamflow drought index (SDI) and standardized streamflow index (SSI) for evaluation of Isfahan drought status. Geol Ecol Landsc. https://doi.org/10.1080/24749508.2024.2359775

Kendall MG (1975) Rank correlation methods. Charles Griffin Book Series, London

Kenabatho PK (2025) Innovative trend analysis of long-term spatial-temporal rainfall patterns over Botswana: implications for water resources management. J Hydrol Reg Stud 58:102217. https://doi.org/10.1016/j.ejrh.2025.102217

Kesgin E, Yaldız SG, Güçlü YS (2024) Spatiotemporal variability and trends of droughts in the Mediterranean coastal region of Türkiye. Int J Climatol. https://doi.org/10.1002/joc.8370

Kherbache N (2020) Water policy in Algeria: limits of supply model and perspectives of water demand management (WDM). Desalin Water Treat 180:141–155

Khoualdia W, Djebbar Y, Hammar Y (2014) Characterization of climate variability: the case of watershed Medjerda (Northeast of Algeria). Rev Sci Technol Synth 29:6–23

Kim HY (2014) Statistical notes for clinical researchers: nonparametric statistical methods: 2. Nonparametric methods for comparing three or more groups and repeated measures. Restor Dent Endod 39:329–332. https://doi.org/10.5395/rde.2014.39.4.329

Kim T, Valdes JB (2003) Nonlinear model for drought forecasting based on a conjunction of wavelet transforms and neural networks. J Hydrol Eng ASCE 8(6):319–328. https://doi.org/10.1061/(ASCE)1084-0699(2003)8:6(319)

Kourat T, Medjerab A (2016) Analyse et cartographie des pluies et l'incidence de leurs variabilité spatiotemporelle sur la délimitation des zones céréalières dans les hautes plaines orientales de l'Algérie. Rev Agric 1:220–229

Kruskal WH, Wallis WA (1952) Use of ranks in one-criterion variance analysis. J Am Stat Assoc 47:583–621. https://doi.org/10.1080/01621459.1952.10483441

Krzywinski M, Altman N (2014) Points of significance: nonparametric tests. Nat Methods 11:467–468. https://doi.org/10.1038/nmeth.2937

Levene H (1960) Robust tests for equality of variances. In: Olkin I, Hotelling H et al (eds) Contributions to probability and statistics: essays in honor of Harold Hotelling. Stanford University Press, Stanford, pp 278–292

Malik A, Tikhamarine Y, Sammen SS, Abba SI, Shahid S (2021) Prediction of meteorological drought by using hybrid support vector regression optimized with HHO versus PSO algorithms. Environ Sci Pollut Res 28:39139–39158. https://doi.org/10.1007/s11356-021-13445-0

Mann HB (1945) Nonparametric tests against trend. Econometrica 245–259

McKee TB, Doesken NJ, Kleist J (1993) The relationship of drought frequency and duration to time scales. In: Proceedings of the 8th conference on applied climatology, Anaheim, California, USA, 17–22 January 1993

Meddi H (2013) Annual variability of precipitation of the Northwest of Algeria. APCBEE Proc 5:373–377

Mishra AK, Singh VP (2011) Drought modelling—a review. J Hydrol 403:157–175. https://doi.org/10.1016/j.jhydrol.2011.03.049

Mohammed T, Al-Amin AQ (2018) Climate change and water resources in Algeria: vulnerability, impact and adaptation strategy. Econ Environ Stud 18(1):411–429

Morid S, Smakhtin V, Bagherzadeh K (2007) Drought forecasting using artificial neural networks and time series of drought indices. Int J Climatol 27:2103–2111. https://doi.org/10.1002/joc.1498

Mostafa-Kara K (2013) État des lieux, bilan et perspectives du défi du changement climatique en Algérie. Éditions Dahlab, Algerie

Mrad D, Djebbar Y, Hammar Y (2018) Analysis of trend rainfall: case of North-Eastern Algeria. J Water Land Dev 36:105–115. https://doi.org/10.2478/jwld-2018-0011

Nalbantis I, Tsakiris G (2009) Assessment of hydrological drought revisited. Water Resour Manag 23:881–897. https://doi.org/10.1007/s11269-008-9305-1

Palmer WC (1965) Meteorological drought. US Department of Commerce Weather Bureau, Washington

Pham MP, Nguyen KQ, Vu GD et al (2022) Drought risk index for agricultural land based on a multi-criteria evaluation. Model Earth Syst Environ 8:5535–5546. https://doi.org/10.1007/s40808-022-01376-9

Quiring SM (2009) Monitoring drought: an evaluation of meteorological drought indices. Geogr Compass 3(1):64–88

Rezaiy R, Shabri A (2025) Integrating wavelet transform and support vector machine for improved drought forecasting based on standardized precipitation index. J Hydroinform 27(2):320–337

Şen Z (2012) Innovative trend analysis methodology. J Hydrol Eng 17:1042–1046

Şen Z, Şişman E, Dabanli I (2020) Wet and dry spell feature charts for practical uses. Nat Hazards 104(3):1975–1986. https://doi.org/10.1007/s11069-020-04257-5

Shafer BA, Dezman LE (1982) Development of a Surface Water Supply Index (SWSI) to assess the severity of drought conditions in snowpack runoff areas (Colorado). In: Proceedings: eastern snow conference, 39th annual meeting, pp. 164–175

Sheskin DJ (2007) Handbook of parametric and nonparametric statistical procedures, 4th edn. Chapman & Hall, London

Taibi S, Meddi M, Souag D, Mahé G (2013) Évolution et régionalisation des précipitations au nord de l'Algérie (1936–2009). IAHS Publ 359:191–197

Tigkas D, Vangelis H, Tsakiris G (2015) DrinC: a software for drought analysis based on drought indices. Earth Sci Inform 8:697–709. https://doi.org/10.1007/s12145-014-0178-y

Tsakiris G, Vangelis H (2004) Towards a drought watch system based on spatial SPI. Water Resour Manage 18:1–12

Tsakiris G, Vangelis H (2005) Establishing a drought index incorporating evapotranspiration. Eur Water 9:3–11

Turhan E, Değerli Şimşek S (2023) Supplementing missing data using the drainage-area ratio method and evaluating the streamflow drought index with the corrected data set. Water 15(3):425. https://doi.org/10.3390/w15030425

Vicente-Serrano SM, Beguería S, López-Moreno JI (2010) A multiscalar drought index sensitive to global warming: the standardized precipitation evapotranspiration index. J Clim 23:1696–1718. https://doi.org/10.1175/2009JCLI2909.1

Wilhite DA, Pulwarty RS (2017) Drought as hazard: understanding the natural and social context. In: Wilhite DA, Pulwarty RS (eds) Drought and water crises: integrating science, management, and policy, 2nd edn. CRC Press, Boca Raton, pp 3–20. https://doi.org/10.1201/b22009

World Meteorological Organization (WMO) (2016) Handbook of drought indicators and indices. (Svoboda M, Fuchs BA) Integrated Drought Management Programme, Series 2, Geneva, Switzerland

Yisehak B, Zenebe A (2021) Modeling multivariate standardized drought index based on the drought information from precipitation and runoff: a case study of Hare watershed of Southern Ethiopian Rift Valley Basin. Model Earth Syst Environ 7:1005–1017. https://doi.org/10.1007/s40808-020-00923-6

Ziari A, Medjerab A (2025) Evaluating drought severity and trends in Northeast Algeria: a comprehensive analysis using the standardized precipitation drought index (ISSP). In: Guerri O, Arab AH, Imessad K (eds) Technological and innovative progress in renewable energy systems, advances in science, technology & innovation. Springer, Cham. https://doi.org/10.1007/978-3-031-71926-4_66